

Spectroscopic Properties of 2,5,8,11-Tetra-*tert*-butylperylene in Polymer Films

J. C. D. Verhagen,[†] M. A. M. J. van Zandvoort,^{*,†} J. M. Vroom,[†] L. B.-Å. Johansson,[‡] and G. van Ginkel[†]

Department of Molecular Biophysics, Debeye Institute, Buys Ballot Laboratory, Utrecht University, P.O. Box 80000, 3508 TA Utrecht, The Netherlands, and Department of Physical Chemistry, University of Umeå, S-90187 Umeå, Sweden

Received: July 3, 1997; In Final Form: September 23, 1997[®]

The spectroscopic properties of 2,5,8,11-tetra-*tert*-butylperylene in poly(vinyl alcohol) have been studied. To this end, the absorption and fluorescence excitation and emission spectra have been measured. The shape of the spectra in poly(vinyl alcohol) is virtually identical with that in propanediol and lipid systems. The Förster radius calculated from the spectra was found to be 3.7 ± 0.3 nm. The natural fluorescence lifetime of 2,5,8,11-tetra-*tert*-butylperylene in poly(vinyl alcohol) was also calculated from the spectra and found to be 5.3 ± 0.2 ns. The fluorescence decay in poly(vinyl alcohol) exhibits monoexponential behavior with a lifetime of 4.5 ± 0.3 ns. It is shown that the fluorescence anisotropy of 2,5,8,11-tetra-*tert*-butylperylene in the polymer matrix does not decay, indicating that its motion is quenched on the time scale of the fluorescence decay. The initial value of the fluorescence anisotropy, $r(0)$, for excitation at 260 nm and emission at 455 nm is -0.16 ± 0.02 while for excitation at 440 nm and emission at 455 nm it is 0.35 ± 0.02 . The fluorescence transition dipole moments relative to the long molecular axis in the plane of the molecule were determined from angle-resolved fluorescence depolarization measurements. This yields an emission dipole moment at 459 nm of $5 \pm 5^\circ$, an excitation dipole moment at 416 nm of $-10 \pm 5^\circ$, and an excitation dipole moment at 256 nm of $80 \pm 5^\circ$.

Introduction

Fluorescent molecules are frequently used as probes in studies of the orientation and dynamics of lipid membranes in order to relate the physical properties of the probes to the biological properties of the membranes. Furthermore they can be used to obtain information about intermolecular energy migration.

Perylene is a widely used membrane probe. The molecule is flat and hydrophobic and is easily incorporated into lipid membranes. Furthermore, perylene is photostable, has a monoexponential decay of its photophysics, and does not change conformation in a lipid bilayer upon electronic excitation.^{1–4} Moreover, it has two almost orthogonal absorption dipole moments in the plane of the molecule, one in the UV and one in the blue.⁵ This property can be exploited in a quantitative characterization of both the orientation and the in-plane and out-of-plane rotations of the molecular plane in the bilayer.^{6–13} In the second place, the two absorption moments can be exploited to obtain additional independent data for use in global target analysis.

2,5,8,11-Tetra-*tert*-butylperylene (TBpe) is a synthetic derivative of perylene, has photophysical properties very similar to perylene, and is sometimes preferable to perylene.^{14–16} In particular, TBpe is more hydrophobic than perylene. Therefore, it is expected that if TBpe is incorporated in a lipid bilayer, all molecules will be found in the middle of the lipid bilayer, while perylene can also intercalate between the lipid chains.^{17,18} Furthermore, the localization of the molecules in the center of the bilayer affords the study of energy migration in a 2-dimensional system.¹⁹

In this work the absorption and fluorescence properties of TBpe in poly(vinyl alcohol) (PVA) film are reported with a

special emphasis on the orientation of the excitation and emission transition dipole moments in the plane of the molecule. Knowledge of these orientations of the transition dipole moments is a prerequisite for studies of TBpe's orientation and rotational motion in the bilayer. Furthermore, energy migration depends on the relative orientation of the emission transition dipole moment of the donor molecule and the absorption transition dipole moment of the acceptor molecule. Consequently, this orientation is determined by the orientation of the transition dipole moments in the donor and acceptor molecules as well as the relative orientation of the donor and acceptor molecules and their reorientational dynamics.²⁰ Thus, knowledge of the orientations of the transition dipole moments in the TBpe molecule is useful for the analysis of energy migration experiments.

We have here chosen to study the photophysical properties of TBpe in a PVA matrix, as we expect that the probes do not change orientation on the fluorescence time scale in the film. Furthermore, the polymer matrix can be macroscopically aligned in a known direction by stretching the film.²¹ This induces a preferential orientation of the probe molecules in the polymer matrix, which is exploited in the determination of the orientation of the transition dipole moments with respect to the long axis of the probe molecule. This will be illustrated in the Theory section. PVA was used because, in contrast to the previously used nitrocellulose (NC),²² it is transparent for both the UV and blue light, needed to excite TBpe at its absorption bands at 259 and 414 nm.

The absorption and fluorescence spectra of TBpe in PVA were found to be in good agreement with those in other media. Subsequently, they were used to determine the Förster radius. The Förster radius is useful in that it allows the determination of the concentrations of TBpe, below which the fluorescence is not influenced by energy migration. The spectra were also used to determine the natural fluorescence lifetime, which in

* Corresponding author.

[†] Debeye Institute.

[‡] University of Umeå.

[®] Abstract published in *Advance ACS Abstracts*, November 1, 1997.

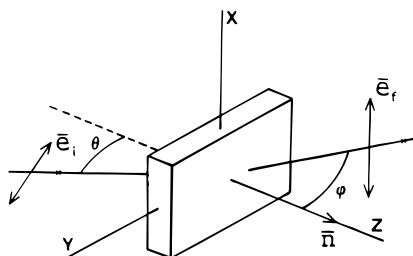


Figure 1. Experimental geometry of an angle-resolved fluorescence depolarization experiment on a stretched polymer film. XYZ = frame of film (Y = stretch direction, Z = normal on film); θ = angle between excitation beam and negative Z ; ϕ = angle between emission direction and Z ; e_i = polarization direction of excitation beam (horizontal); e_f = polarization direction of emission beam (horizontal or vertical).

combination with the fluorescence decay time yielded the quantum yield.

Next, the spatial distribution of TBpe molecules in the PVA matrix was determined by confocal imaging fluorescence microscopy. In addition, the average fluorescence lifetime of TBpe was determined at various places in the PVA film.

Finally, the presence of rotational motions and intermolecular energy migration was monitored by using time-resolved anisotropy techniques. The anisotropy was constant in time, which showed that the TBpe was immobilized and that there was no energy migration between the molecules, wherefore the system of TBpe in PVA can be used to determine the orientation of the excitation and emission transmission moments of TBpe in the molecule. The fluorescence anisotropy was used to determine the angle between the transition dipole moments; angle-resolved fluorescence depolarization (AFD) measurements were employed to determine the angle the transition dipole moments made with the long axis of the TBpe molecule.

Theory

We will outline the theory necessary to extract the orientations of the transition dipole moments in the molecular frame of TBpe from AFD measurements in stretched polymer films, and we will show how to determine the difference angle between the emission and excitation dipole moment from the steady-state fluorescence anisotropy in an immobilized isotropic medium.

Steady-State AFD of Molecules in Stretched Films. The geometry of the AFD measurements is shown in Figure 1. A stretched film with the stretch direction horizontal is illuminated with horizontally polarized light. The emission light is detected in the horizontal and vertical polarization direction for several values of θ (the angle between the direction of the exciting beam and the normal on the film) and ϕ (the angle between the direction of the detected emission light and the normal on the film). Under these experimental conditions, the fluorescence intensities I_{hv} and I_{hh} and their ratio, $R_e = (I_{hv}/I_{hh})$, are given by the following expressions:²³

$$\begin{aligned} I_{hv} &= (k/9)(1 + 2S_\mu - S_\nu - 2G_0 - 3(S_\nu - G_0 + G_2) \sin^2 \theta) \\ I_{hh} &= (k/9)(1 + 2S_\mu + 2S_\nu + 4G_0 - 3(S_\mu + 2G_0) \sin^2 \theta - \\ &\quad 3(S_\nu + 2G_0) \sin^2 \phi + 3(G_2 + 3G_0) \sin^2 \theta \sin^2 \phi - \\ &\quad 3G_1 \sin 2\theta \sin 2\phi) \quad (1) \end{aligned}$$

The terms in this expression have the following meanings: I_{if} is the intensity of the fluorescence light with polarization direction f , caused by illuminating the sample with a light beam with polarization direction i (see also Figure 1). k is a constant determined by the excitation light intensity and probe concentra-

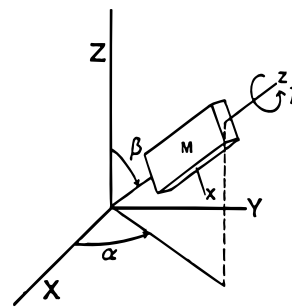


Figure 2. Definition Euler angles: M = molecule, XYZ = laboratory frame, xyz = molecule frame; α = angle between projection molecule z -axis on XY -plane and the X -axis; β = angle between the z -axis and the Z -axis; γ = angle that the x -axis has rotated around the z -axis.

tion.

$$S_\mu = \sum_{i=-2}^2 \langle D_{0i}^2(\Omega_{sm}) \rangle D_{i0}^2(\Omega_\mu) \quad (2)$$

$$S_\nu = \sum_{j=-2}^2 \langle D_{0j}^{2*}(\Omega_{sm}) \rangle D_{j0}^{2*}(\Omega_\nu) \quad (3)$$

$$G_k = \sum_{i,j=-2}^2 \langle D_{kj}^{2*}(\Omega_{sm}) D_{ki}^2(\Omega_{sm}) \rangle D_{j0}^{2*}(\Omega_\nu) D_{i0}^2(\Omega_\mu) \quad (4)$$

$D_{mn}^L(\Omega)$ is a Wigner rotation matrix element.²⁴ Ω_μ ($\alpha_\mu, \beta_\mu, \gamma_\mu$) and Ω_ν ($\alpha_\nu, \beta_\nu, \gamma_\nu$) are the Euler angles of respectively the absorption and emission dipole moments in the molecular frame (see also Figure 2). Ω_{sm} is the Euler angle between the director of the TBpe molecule and the director of the film. $\langle X_{sm} \rangle$ is the ensemble average $\int d\Omega_{sm} f(\Omega_{sm}) X(\Omega_{sm})$ of $X(\Omega_{sm})$ over the distribution function $f(\Omega_{sm})$. $f(\Omega_{sm})$ is the orientational distribution function of the TBpe molecules.

Equations 2–4 express the separation of the geometrical factors θ and ϕ dictated by the experimental setup from the molecular properties, the order parameters S_μ and S_ν , and the correlation functions G_k .

Since all five experimental parameters S_μ, S_ν, G_0, G_1 , and G_2 appear in the expression for R_e , they can be determined in an AFD experiment. The orientational distribution, $f(\Omega_{sm})$, and the orientation of the transition dipole moments in the molecular frame, β_μ and β_ν , are determined from these five parameters with a Marquard least-squares algorithm, as explained below.

Interpretation of the Experimental Parameters. In the following we will limit ourselves to the case of quenched reorientational motions. We shall also assume the orientational distribution of the pigments in the polymer matrix to be either isotropic (in an unstretched film) or uniaxially symmetric around the stretch direction (in a stretched film)²² so that $G_k = G_{-k}$. Equation 1 indicates that a fluorescence depolarization experiment yields a maximum of five independent parameters, S_μ, S_ν, G_0, G_1 , and G_2 . These experimental parameters contain all the accessible molecular information. The question now arising is how to extract the information on orientational distribution and the transition dipole moments from the five experimental parameters. TBpe is a planar ring with the transition dipole moments in the plane of the ring. The absorption and emission dipole moments are completely defined by the Euler angles β_μ and β_ν with the long axis of the TBpe molecule in the ring (Figure 8).

In the situation of quenched reorientational motions, the correlation functions G_k can be expressed in the order parameters

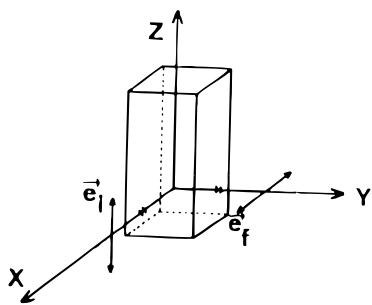


Figure 3. The 90° depolarization experiment with cuvette: X = axis excitation beam; Y = axis detected emission light; e_i and e_f = polarization directions of respectively absorption and emission light.

of rank $L = 2$ and $L = 4$, using the Clebsch Gordon series^{24–26} and the Euler angles of the transition dipole moments.

The orientational information in the experimental parameters (S_μ , S_ν , G_0 , G_1 , and G_2) is expressed in up to 25 second rank and 81 fourth rank order parameters. However, many of these are zero for reasons of symmetry.^{27–29} For films stretched uniaxially along the Z -axis, the distribution of the planar pigments is invariant under rotations around this axis, possesses mirror symmetries in the XY - and XZ -plane of the film, and, moreover, is invariant to reflections in the xz - and yz -molecular frames. Consequently, only five nonzero order parameters remain:

$$\langle P_2 \rangle = \langle D_{00}^2 \rangle, \langle P_4 \rangle = \langle D_{00}^4 \rangle, \langle D_{02}^2 \rangle, \langle D_{02}^4 \rangle, \text{ and } \langle D_{04}^4 \rangle$$

As we need two parameters for the angles of the transition moments, there are in total seven parameters to extract from the five experimentally available parameters S_μ , S_ν , G_0 , G_1 , and G_2 . In a polymer a good choice for the interpretation of the data is the use of the first three parameters, $\langle P_2 \rangle$, $\langle P_4 \rangle$, and $\langle D_{02}^2 \rangle$.³⁰ The smoothest possible orientational distribution function $f(\Omega_{sm})$ that is consistent with these three order parameters may be reconstructed with the maximum entropy formalism given by van Gurp et al.³⁰ and Levine et al.³¹

$$f(\Omega_{sm}) = A \exp\{\lambda_2 P_2(\Omega_{sm}) + \lambda_4 P_4(\Omega_{sm}) + \epsilon [D_{02}^2(\Omega_{sm}) + D_{0-2}^2(\Omega_{sm})]\} \quad (5)$$

In this equation A is a normalization constant. λ_2 , λ_4 , and ϵ are variables whose values are uniquely related to the three order parameters.

Any order parameter $\langle X \rangle$ can be calculated from this equation with the above expression, since $\langle X \rangle = \int d\Omega_{sm} f(\Omega_{sm}) X(\Omega_{sm})$. This approach now expresses the five experimental parameters S_μ , S_ν , G_0 , G_1 , and G_2 in terms of three variables, describing the orientational distribution of the molecules relative to the stretch direction (λ_2 , λ_4 , and ϵ), and two variables, β_μ and β_ν , defining the orientation of the transition dipole moments relative to the in-plane z -axis of the molecular ring, using eqs 2–5.

Steady-State Fluorescence Anisotropy of Molecules in Immobilized Solutions. The geometry for fluorescence anisotropy measurements is shown in Figure 3. The sample is illuminated with vertically polarized light, and the fluorescence light is detected for both the horizontally and vertically polarized emission light in a direction perpendicular to the excitation beam.

In isotropic solutions S_μ and S_ν are equal to zero, since the fluorophores have no preferential orientation. An additional consequence of the random orientation is that the three correlation functions are equal and are only determined by the difference angle $\beta_{\mu-\nu}$ between the absorption and emission

transition dipole moments in the molecular frame.²⁷

$$G_0 = G_1 = G_2 = 1/5 P_2(\cos(\beta_{\mu-\nu})) \quad (6)$$

The fluorescence anisotropy r_{ss} is defined by

$$r_{ss} = \frac{I_{vv}/I_{vh} - 1}{I_{vv}/I_{vh} + 2} \quad (7)$$

In this equation the subscripts denote the polarization directions of the exciting and emitted light in the laboratory frame. The anisotropy in an isotropic immobilized system is related to $\beta_{\mu-\nu}$ by the following equation:³²

$$r_{ss} = 2/5 P_2(\cos(\beta_{\mu-\nu})) \quad (8)$$

Thus, fluorescence anisotropy experiments on unstretched films yield only the difference angle between the absorption and emission dipole moments in the molecular frame.

Experimental Section

TBpe was synthesized and used as described previously.³³ Completely hydrolyzed PVA with an average weight of about 100 was obtained from Aldrich Chemie and cleaned from side products (acidic traces and residual acetyl groups) by the modified ethanol extraction method described van Zandvoort et al.³⁴ Dimethyl sulfoxide (DMSO) of analytical grade was obtained from J.T. Baker Chemicals B.V. and used without further purification. Propane-1,2-diol (purity >99.5%) was obtained from Merck and obtained without further purification. Spectrophotometric grade glycerol was obtained from Aldrich.

A PVA solution in DMSO was prepared under nitrogen atmosphere by adding 0.5 g of cleaned PVA powder to 6 mL of DMSO and heating this mixture to 80 °C under continuous magnetic stirring until an optically clear solution was obtained. The PVA–DMSO solution was cooled and then mixed with 0.1 μ mol of TBpe dissolved in a small amount of DMSO, resulting in a concentration of 0.2 μ mol of TBpe/g of PVA. This mixture was stirred for 15 min. Films were prepared from this solution by pouring it out on a glass plate and drying in the dark for 40 h under a continuous nitrogen stream. The film was cut from the glass plate. To stretch a PVA film, the film was heated to 80 °C, stretched, left some time to stabilize in the stove, and stretched again until it reached 3 or 4 times its original length. The refractive index of both stretched and unstretched PVA films was measured with an Abbe refractometer and found to be 1.52 ± 0.02 with a double refraction within the experimental error. Both stretched and unstretched films were pressed between quartz plates using glycerol to improve optical contact. Finally, the samples were sealed at the edges with glue.

Absorption spectra were measured with SLM-Aminco DW2000 spectrophotometer (bandwidth 2 nm). The absorptions were deliberately kept below 0.2 to prevent reabsorption. The fluorescence excitation and emission spectra were measured with a SLM-Aminco SPF 500 spectrofluorimeter. For solutions the standard 90° setup was used. Polymer films were mounted in a special holder, so that their surface made an angle of 45° with the incident and the emitted beam in such a way that the reflection from the incident beam was 180° from the emission detector. Bandwidths were 2 nm for solutions and 5 nm for films.

Fluorescence Intensity and Fluorescence Lifetime Images. The fluorescence intensity and fluorescence lifetime images were measured using the confocal scanning fluorescence microscope

(CSFLM), described by Sytsma and co-workers.³⁵ The TBpe molecules were excited using two-photon absorption³⁶ with a titanium–sapphire laser (Spectra Physics, Model 3960) pumped by a 10 W argon ion laser. The repetition frequency is 82 MHz, full width at half-maximum (fwhm) of the pulses being 70 fs. The time-averaged power of the laser is between 1 and 1.5 W. The power on the sample was reduced to several milliwatts using neutral density filters.

A wavelength of 705 nm was selected, which due to two-photon excitation resulted in an effective wavelength 353 nm.³⁵ The use of two-photon excitation has the advantage that it reduces the bleaching outside the focus of the microscope.

The emission light from the sample was collected by an objective and detected through a 464 ± 6 nm interference filter, a GG455 broad-band filter, and a 420 nm cutoff filter and detected with a 0.8 ns risetime photomultiplier tube (PMT, Hamamatsu R1894, selected for photon counting).

The fluorescent lifetime for each pixel is measured by single-photon counting in two adjacent time gates after the laser pulse.³⁵ After the full scan was performed, two images were calculated by taking the sum and the ratio of the total number of counts of the two time windows. The sum is directly proportional to the fluorescence intensity of a pixel in the sample. The average fluorescence lifetime is determined from the ratio.³⁵

Fluorescence Lifetime Decay Behavior in Films. The microscope was also used to record the fluorescence lifetime curves within a single volume element of TBpe in PVA film by means of time-correlated single-photon counting (TCSPC). A pulse picker is used to lower the repetition frequency of the excitation light from 82 to 8 MHz to avoid pileup. The signal of the PMT is used to provide a start pulse for a time-to-amplitude converter (TAC). A signal from a photodiode monitoring the laser is used to provide the stop pulse of the TAC. The output of the TAC is read by a multichannel board (EG&G Ortec 916A, 2048 channels, channel width 0.0264 ns) which is controlled by multichannel analyzer emulation software on a PC. The fluorescence lifetime decays are fitted with a sum of exponentials.

Time-Resolved Fluorescence Anisotropy. The time-resolved fluorescence anisotropy measurements on solutions were carried out in Daresbury Laboratory (UK) using synchrotron radiation as a tunable pulsed light source with 300 MHz repetition frequency.³⁷ The excitation wavelength was selected with a monochromator with bandwidth between 0.1 and 3 nm and a Glan-Taylor polarizer to select vertically polarized light. The emitted light was detected through an IF 480 and FF 470 filter and an emission sheet polarizer with its polarization direction horizontal or vertical. The pulse profile was measured using a blank film as scatterer. A Philips XP2020Q photomultiplier tube was used for detection. The decay curves were analyzed with a reiterative convolution algorithm using a nonlinear least-squares Marquard procedure.

Steady-State Fluorescence Anisotropy. The steady-state fluorescence anisotropy excitation and emission spectra in propane-1,2-diol at -9°C were measured with a SLM-Aminco SPF 500 spectrofluorimeter with its standard anisotropy device, using 90° geometry. The correction factor ($I_{\text{hh}}/I_{\text{hv}}$) accounting for the difference in response of the emission line to horizontally and vertically polarized light was determined on the sample.

Steady-State Angle Resolved Fluorescence Depolarization. Steady-state AFD experiments were carried out on the setup as described by van Gurp et al.²⁷ The excitation light was selected to be either 258 or 416 nm for PVA films. The 258 nm wavelength was selected with an 258 ± 5 nm interference filter and an UG5 broad-band filter. The 416 nm wavelength was

selected with a 416 ± 4 nm interference filter and two UG3 broad-band filters. The exciting light was polarized with a horizontally aligned Glan-Taylor prism. The emission light was detected through a 464 ± 6 nm interference filter, a GG455 broad-band filter, and a 420 nm cutoff filter. Either horizontally or vertically polarized emitted light was detected with a sheet polarizer. The measurements were done for 60 different angles of excitation and emission. The correction factor ($I_{\text{hh}}/I_{\text{hv}}$) to account for the difference in response of the emission line to horizontally and vertically polarized light was determined with a 90° setup on a dilute solution of TBpe in ethanol. The R_e values for both wavelengths were analyzed simultaneously with a reiterative convolution algorithm using a nonlinear least-squares Marquard procedure. The values for $\beta_{\mu=416}$, $\beta_{\mu=256}$, λ_2 , λ_4 , and ϵ were allowed to vary, while the value for β_v was kept fixed. By doing this for several values of β_v , the χ^2 minima could be found.³⁷

Natural Lifetime and Fluorescence Lifetime. The natural lifetime τ_0 is the lifetime of a fluorescent probe in the absence of nonradiative decay processes. The natural lifetime of TBpe is determined from the absorption and emission spectra of TBpe in PVA/DMSO solution (1.5×10^{-5} M TBpe/DMSO, 0.08 g of PVA/mL of DMSO). The spectra were not measured in PVA film itself due to the errors introduced by the low absorption in a thin film. The natural lifetime was determined by using the following equation:³⁸

$$\frac{1}{\tau_0} = 2.88 \times 10^{-9} n^2 \frac{\int F(\lambda) \lambda^{-2} d\lambda}{\int F(\lambda) \lambda d\lambda} \int \frac{\epsilon(\lambda)}{\lambda} d\lambda \quad [\text{s}^{-1}] \quad (9)$$

In this expression n is the refractive index, $F(\lambda)$ the emission spectrum as a function of the wavelength, and $\epsilon(\lambda)$ the absorption as a function of the wavelength.

The observed average fluorescence lifetime, $\langle\tau\rangle$, is determined from the decay of the total fluorescence intensity. The quantum yield is determined from the ratio $\langle\tau\rangle/\tau_0$.

Förster Radius. The Förster radius, R_0 , is the distance between two molecules for which the probability of decay of the excited state of a fluorescent molecule due to energy migration from the first to the second molecule and the probability of decay due to fluorescence decay of the molecule are equal. The Förster radius of TBpe was determined from the absorption and emission spectra of TBpe in PVA/DMSO (15 μg of TBpe/mL of DMSO, 1 mg of PVA/mL of DMSO) solution, using the following expression:^{34,39–44}

$$R_0^6 = 8.79 \times 10^{-25} \frac{2}{3} \frac{1}{n^4} \frac{\int F(\lambda) \epsilon(\lambda) \lambda^2 d\lambda}{\int F(\lambda) \lambda^{-2} d\lambda} \quad [\text{cm}^6] \quad (10)$$

In this expression n is the refractive index, $F(\lambda)$ the emission spectrum as a function of the wavelength, and $\epsilon(\lambda)$ the absorption as a function of the wavelength. The constant $2/3$ arises from the average value of the orientation factor κ^2 in isotropic systems.^{40,43}

Results

Absorption, Excitation, and Emission Spectra. In Figure 4 the absorption, excitation, and emission spectra of TBpe in propane-1,2-diol are shown. Spectra similar of shape are obtained from TBpe in DMSO, DMSO/PVA, and PVA films. The absorption maxima of TBpe in propane-1,2-diol are 257, 391, 411, and 436 nm with an error of 1 nm. In DMSO and PVA/DMSO solution the blue absorption maxima are 393, 414,

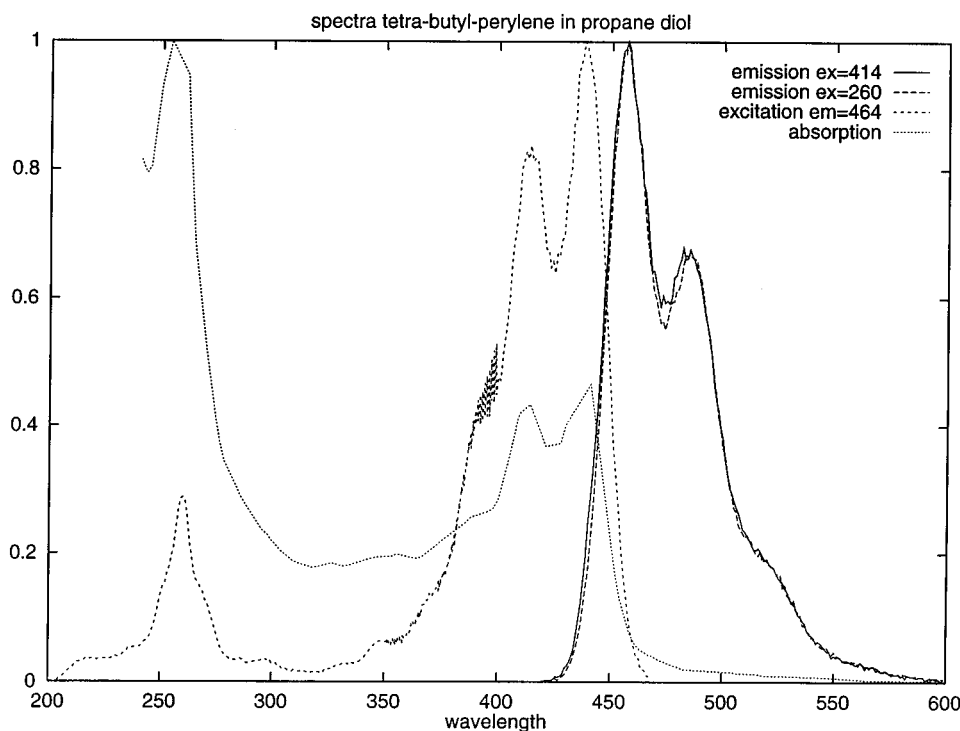


Figure 4. Absorption, excitation, and emission of tetrabutylperylene in propane-1,2-diol.

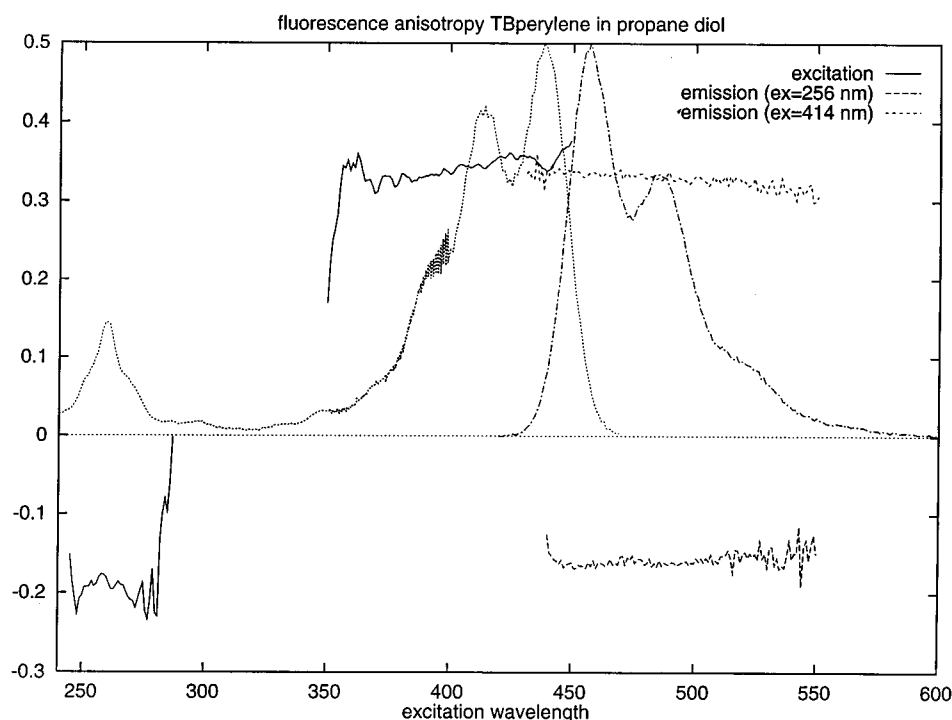


Figure 5. Fluorescence anisotropy of tetrabutylperylene.

and 439 nm with an error of 1 nm. The UV absorption maximum cannot be measured, due to the absorption of DMSO in this spectral region. In stretched and unstretched PVA films the absorption maxima are 259, 391, 414, and 440 nm with an error of 3 nm. In all systems the excitation spectrum coincides with the absorption spectrum, independent of the emission wavelength.

The emission maxima in propane-1,2-diol are 457 and 485 nm. In DMSO and PVA/DMSO the emission maxima are 459 and 487 nm, while the emission maxima in PVA film are located at 459 and 485 nm. The error in all the emission peak positions is 1 nm. The emission spectrum in both propane-1,2-diol and PVA film is independent of the excitation wavelength. Again,

the emission spectrum in DMSO and PVA/DMSO for the UV excitation wavelength could not be measured due to the absorption of DMSO in the UV.

The natural fluorescence lifetime of TBpe as calculated from the absorption and emission spectrum in PVA/DMSO solution (0.08 g of PVA/mL of DMSO) with use of eq 9 is found to be 5.3 ± 0.3 ns.

The Förster radius of TBpe in PVA/DMSO solution is calculated from the spectra using eq 10 and a refractive index of 1.52. The obtained value is 3.7 ± 0.3 nm.

Fluorescence Steady-State Anisotropy. The excitation anisotropy spectrum of TBpe in propane-1,2-diol at -9 °C for an emission wavelength of 455 nm is shown in Figure 5. We

TABLE 1: Measured Fluorescence Lifetimes (τ) of TBpe

TBpe in	τ^a (ns)
DMSO solution (10 μ mol/L)	4.56
PVA/DMSO solution (10 μ mol/L)	4.50
unstretched PVA film (0.6 μ mol/g)	4.60
stretched PVA film (0.6 μ mol/g)	4.24

^a The error in the lifetime is 0.05 ns.

TABLE 2: Limiting Anisotropy, r_0 , of TBpe^a

solvent	blue (414 nm)	UV (265 nm)
ethanol	0.35	-0.20
PVA/DMSO	0.35	-0.16
PVA	0.36	-0.16

^a The error in the limiting anisotropy is 0.01 for the blue band and 0.02 in the UV band.

TABLE 3: Results of AFD Experiments^a

	3 \times stretched		4 \times stretched	
	a	b	a	b
λ_2	0.41	-0.11	0.72	-0.73
λ_4	0.0	0.0	0.0	0.0
ϵ	0.11	0.36	-0.5	0.33
β_v	5	95	10	95
$\beta_{\mu=416}$	-15	75	-10	80
$\beta_{\mu=256}$	75	170	80	175
$\langle P_2 \rangle$	0.09	-0.03	0.15	-0.14
$\langle D_{02}^2 \rangle$	0.02	0.06	-0.07	0.06
$\langle P_4 \rangle$	0.00	0.00	0.00	0.00
$\langle D_{02}^4 \rangle$	0.00	0.00	0.00	0.00
$\langle D_{04}^4 \rangle$	0.00	0.00	0.00	0.00

^a The errors in the angles is 5° and λ_2 , λ_4 , and ϵ is 0.07 and in the order parameters 0.01.

find an anisotropy plateau of $r_{ss} = -0.18 \pm 0.02$ for excitation wavelengths between 255 and 280 nm and an anisotropy plateau of $r_{ss} = 0.36 \pm 0.02$ for excitation wavelengths in the range from 370 to 450 nm. The emission anisotropy spectrum (Figure 5) for excitation at 260 nm has a plateau of -0.17 ± 0.04 between 450 and 530 nm, while for an excitation wavelength of 414 nm a plateau of 0.34 ± 0.02 in the same emission spectral range is found.

Fluorescence Intensity and Lifetime Image of Film. The fluorescence intensity images for both the stretched and the unstretched PVA film show that intensity is homogeneous over the whole film. The same holds for the fluorescence lifetime images. The measured fluorescence lifetimes, including those in films, are shown in Table 1. In all the media studied the fluorescence intensity decay was monoexponential, the lifetime being the same within the experimental error.

Time-Resolved Anisotropy. The fluorescence anisotropy at time zero for TBpe in ethanol, PVA/DMSO, and PVA film is given in Table 2. The value is 0.35 ± 0.01 for the blue and -0.16 ± 0.02 for the UV absorption band. The fluorescence anisotropy of TBpe in PVA film is constant within the fluorescence lifetime window.

Angle-Dependent Fluorescence Depolarization. AFD measurements were done on TBpe in PVA film, stretched to 3 times and 4 times its original length. The obtained parameters are shown in Table 3. The χ^2 fit of the AFD data yields two separate χ^2 minima A and B for both cases (see respectively Figures 6 and 7).

Solution A has a maximum in the distribution function $f(\beta)$ along the stretch direction ($\beta = 0^\circ$) (Figure 6). The emission transition moment within the molecular frame makes an angle with the long molecular axis of $5 \pm 5^\circ$. The excitation transition

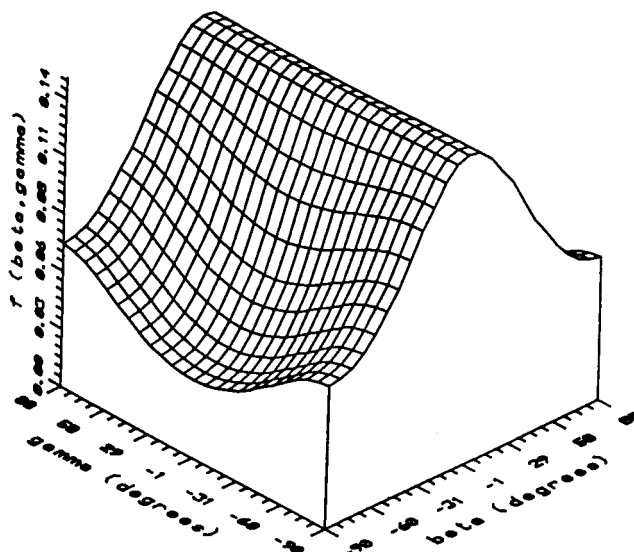


Figure 6. Distribution function $f(\beta)$ of TBpe in PVA matrix (4 \times stretched). Solution A.

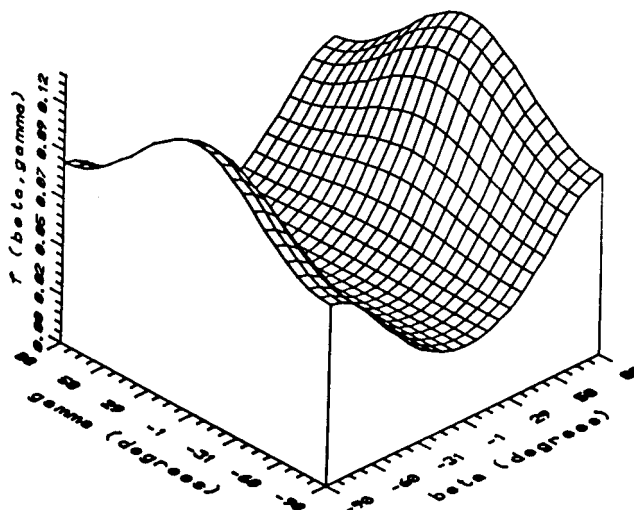


Figure 7. Distribution function $f(\beta)$ of TBpe in PVA matrix (4 \times stretched). Solution B.

moments for excitation at 416 and 256 nm make angles of respectively $-10 \pm 5^\circ$ and $80 \pm 5^\circ$ with the long axis of the molecule.

Solution B has a maximum in the distribution function $f(\beta)$ perpendicular to the stretch direction ($\beta = 90^\circ$) (Figure 7). The emission transition moment within the molecular frame makes an angle with the long molecular axis of $85 \pm 5^\circ$. The excitation transition moments for excitation at 416 and 256 nm make angles of respectively $-75 \pm 5^\circ$ and $10 \pm 5^\circ$ with the long axis of the molecule.

We will discuss the relevance of these two solutions in the Discussion section.

Discussion

The absorption, excitation, and emission spectra in propane-1,2-diol, DMSO, PVA/DMSO, and PVA films are almost identical, with shifts of 2 nm or less. Furthermore, the absorption and excitation spectra coincide, and the shape of the emission spectrum is independent of the excitation wavelength in all the systems studied. Therefore, we can conclude that only a single absorbing and fluorescing species of TBpe exists, and we can also exclude the presence of TBpe aggregates.^{34,45-49}

The natural lifetime of TBpe was found to be 5.3 ns while the fluorescence lifetime was measured to be 4.5 ns, giving a

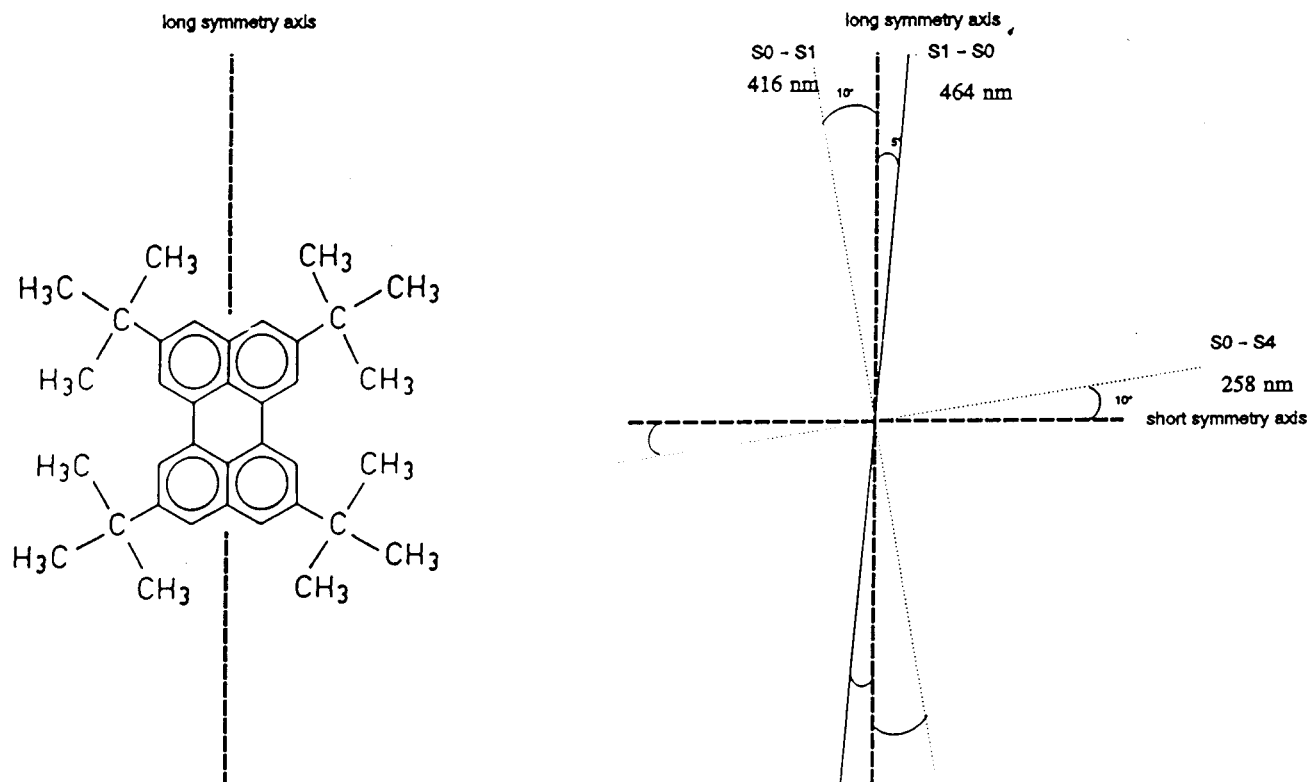


Figure 8. TBpe with its emission and excitation transition dipole moments.

value of 0.85 ± 0.09 for the quantum yield of TBpe in PVA–DMSO. Taking into account the similarity of the spectra in all media and the independence of the fluorescence lifetime in all media studied, it is reasonable to assume that the quantum yield of TBpe in all media is similar. Kalman et al. had found a quantum yield of TBpe in dioleoylglycerophosphocholine (DOPC) of 0.88 ± 0.07 , which lies within the experimental error of our measurements.¹⁸

The fluorescence intensity and lifetime images of TBpe in both stretched and unstretched PVA films are the same across the whole film, implying that TBpe is uniformly distributed over the film and that no clusters of TBpe are present. Such a homogeneous probe distribution is essential for the interpretation of the AFD measurements; it furthermore shows that TBpe in PVA is a suitable system for energy migration studies.⁵⁰

To check whether there is any energy migration in the films used, we calculated the concentration of TBpe in PVA for which the distance between the molecules is equal to the Förster radius. For a density of PVA of 1 kg/L, that concentration would be 8 μmol of TBpe/g of PVA. The concentration we used in our films was 0.2 μmol of TBpe/g of PVA, which is well below this value. Therefore, there should be no fluorescence anisotropy decay due to energy migration visible in the film. As expected, the time-resolved anisotropy measurements in PVA films do not show any decay within this time window. Thus, there is not only no energy migration but also no reorientational dynamics within the time window of the fluorescence lifetime. The steady-state anisotropies in propane-1,2-diol at -9°C are the same as the $r(0)$ in the time-resolved measurements, which supports the absence of energy migration and dynamics once more.

We have used excitation wavelengths of 258 and 416 nm and an emission wavelength of 464 nm for the time-resolved and AFD measurements. While previously in NC²² this was not possible due to the high absorption of NC in the UV, now both wavelengths can be excited. This enables us, due to

combined analysis, to more accurately determine the absolute orientation of both excitation dipole moments in the molecular frame. Furthermore, both wavelengths lie well within the spectral range where the anisotropy is constant, as we have indicated in the Results section and Figure 5. On this basis, we conclude that only one electronic transition is excited at these wavelengths. The $r(0)$ is 0.35 ± 0.02 for the blue band. This gives an angle of $17 \pm 4^\circ$ between the blue excitation transition moment and the emission moment. The $r(0)$ for the UV absorption band is -0.16 ± 0.02 . This results in an angle of $83 \pm 7^\circ$ between the UV excitation transition moment and the emission transition moment. The values for r_{ss} are the same within experimental error.

The solutions A and B from the AFD data analysis described in the Results section are the same upon a 90° rotation of the symmetry axis. This can be seen from the shape of the distribution functions (Figures 6 and 7) and the values of β_μ and β_ν in Table 3. The transition moments of result B are simply those of A plus 90° . Also, if the coordinate system of A is rotated over 90° , the order parameters of result A are transformed into the order parameters of result B.

Result A has most molecules oriented along the stretch direction ($\beta = 0$) and result B perpendicular to the stretch direction ($\beta = 90^\circ$). As it is logical to assume that the long axis is preferentially oriented along the stretch direction, we assume that result A uses the long axis of the TBpe molecule as symmetry axis and result B the short axis. Figure 8 shows how the transition moments are positioned in the molecule with the emission transition moment at $5 \pm 5^\circ$ with respect to the long molecular symmetry axis, the 416 nm excitation transition moment at $-10 \pm 5^\circ$, and the 256 nm excitation transition moment at $80 \pm 5^\circ$ with respect to the long molecule axis. The difference angle between the excitation transition moments and the emission moment from these values are 15° for 416 nm and 75° for 256 nm, which are within experimental error equal to the values found from the anisotropy measurements.

These results fit in with those found by some of us for the blue band of TBpe in NC.²² There, however, one could not see the UV band because of the UV absorption of NC.

Finally, it should be noted that the ordering of Tbpe in the PVA matrix is quite low. This, however, should not come as a surprise, since such low ordering effects in PVA were found before for various other probes such as chlorophyll *a*, pheophytin *a*, eosin-5-maleimide, and 1,5-I-IAEDANS.^{38,51} We want to stress that even such low ordering enables us to determine the orientation of the transition dipole moments in the molecular frame.

References and Notes

- (1) Johansson, L. B.-Å. *Chem. Phys. Lett.* **1986**, *118*, 516.
- (2) Barkley, A. A.; Kowalczyk, L.; Brand, J. *Photochem.* **1981**, *9*, 219.
- (3) Christensen, R. L.; Drake, R. C.; Phillips, D. J. *Phys. Chem.* **1986**, *90*, 5960.
- (4) Tachikawa, H.; Faulkner, L. R. *Chem. Phys. Lett.* **1976**, *39* (3), 436.
- (5) Johansson, L. B.-Å. *J. Chem. Soc., Faraday Trans.* **1990**, *86* (12), 2103.
- (6) van der Heide, U. A. A fluorescence depolarization study of crossbridge rotation in skeletal muscle. Thesis University Utrecht, Utrecht, 1993.
- (7) Labhart, H.; Pantke, E. R. *Chem. Phys. Lett.* **1973**, *23* (4), 482.
- (8) Zinsli, P. E. *Chem. Phys.* **1977**, *20*, 299.
- (9) Lakowicz, J. R.; Knutson, J. R. *Biochemistry* **1980**, *19*, 905.
- (10) Lakowicz, J. R.; Cherek, H.; Maliwal, B. P. *Biochemistry* **1985**, *24*, 376.
- (11) Sasaki, T.; Hirota, K.; Yamamoto, M.; Nishijima, Y. *Bull. Chem. Soc. Jpn.* **1987**, *60*, 1165.
- (12) Piston, D. W.; Bilash, T.; Ratton, E. J. *Phys. Chem.* **1989**, *93*, 3963.
- (13) Szubiakowski, J.; Balter, A.; Nowak, W.; Kowalczyk, A.; Wiśniewski, K.; Wierzbowska, M. *Chem. Phys.* **1996**, *208*, 283.
- (14) Kalman, B.; Clarke, N.; Johansson, L. B.-Å. *J. Phys. Chem.* **1989**, *93*, 4608.
- (15) Johansson, L. B.-Å.; Molotovskiy, J. G.; Bergelson, L. D. *J. Am. Chem. Soc.* **1987**, *109*, 7374.
- (16) De Backer, S.; Negri, M. R.; De Feyter, S.; Dutt, G. B.; Ameloot, M.; De Schryver, F. C.; Müllen, K.; Holtrup, F. *Chem. Phys. Lett.* **1995**, *233*, 538.
- (17) Kalman, B.; Johansson, L. B.-Å.; Lindberg, M.; Engström, S. *J. Phys. Chem.* **1989**, *93*, 8371.
- (18) van Zandvoort, M. A. M. J.; Gerritsen, H. C.; van Ginkel, G.; Levine, Y. K. *J. Phys. Chem. B* **1997**, *101*, 4149.
- (19) Johansson, L. B.-Å.; Engström, S.; Lindberg, M. *J. Chem. Phys.* **1992**, *96*, 3844.
- (20) Knoester, J.; van Himbergen, J. E. *J. Chem. Phys.* **1984**, *81*, 4380.
- (21) Michl, M.; Thulstrup, E. W. *Spectroscopy with Polarized Light; Solute Alignment by Photoselection in Liquid Crystal Polymers and Membranes*; VCH Publishers: New York, 1986.
- (22) van Zandvoort, M. A. M. J.; Lettinga, P. M.; van der struijf, C.; van Ginkel, G.; Levine, Y. K. *J. Fluoresc.* **1994**, *4*, 83.
- (23) Samori, B.; Thulstrup, E. W., Eds. *Polarized Spectroscopy of Ordered Systems*; Kluwer Academic Publishers: Dordrecht, 1988; p 455.
- (24) Rose, M. E. *Elementary Theory of Angular Momentum*; Wiley: New York, 1957.
- (25) Particle Data Group, *Rev. Mod. Phys.* **1976**, *46*, s36.
- (26) Luckhurst, G. R.; Gray, G. W., Eds. *The Molecular Physics of Liquid Crystals*; Academic Press: New York, 1979; p 51vv.
- (27) van Gorp, M.; van Ginkel, G.; Levine, Y. K. *J. Polym. Sci. B* **1988**, *26*, 1613.
- (28) van Gorp, M.; van Ginkel, G.; Levine, Y. K. *J. Chem. Phys.* **1989**, *8*, 4095.
- (29) van Gorp, M.; Levine, Y. K. *Chem. Phys. Lett.* **1991**, *180*, 349.
- (30) Samori, B.; Thulstrup, E. W., Eds. *Polarized Spectroscopy of Ordered Systems*; Kluwer Academic Press: Dordrecht, 1988; p 455vv.
- (31) Miller, W. H. Ed. *Modern Theoretical Chemistry III Dynamics of Molecular Collisions*; Plenum: New York, 1975.
- (32) Szabo, A. J. *Chem. Phys.* **1984**, *81*, 150.
- (33) Johansson, L. B.-Å.; Molotovskiy, J. G.; Bergelson, L. D. *J. Am. Chem. Soc.* **1987**, *109*, 7374.
- (34) van Zandvoort, M. A. M. J.; Wróbel, D.; Scholten, A. J.; de Jager, D.; van Ginkel, G.; Levine, Y. K. *Photochem. Photophys.* **1993**, *58*, 600.
- (35) Sytsma, J.; Vroom, J.; Gerritsen, H.; Levine, Y. K. *SPIE Proc.* **1995**, *2412*, 110.
- (36) Yu, J.-A.; Nocera, D. G.; Leroi, G. E. *Chem. Phys. Lett.* **1990**, *167* (1, 2), 85.
- (37) Munro, I. H.; Schwantner, N. *Nucl. Instrum. Methods* **1983**, *208*, 819.
- (38) van der Heide, U. A.; Orbons, B.; Gerritsen, H. C.; Levine, Y. K. *Eur. Biophys. J.* **1992**, *21*, 263.
- (39) Birks, J. B. *Photophysics of Aromatic Molecules*; Wiley-Interscience: London, 1970.
- (40) Förster, Th. *Radiat. Res. Suppl.* **1960**, *2*, 326.
- (41) Förster, Th. *Ann. Phys.* **1948**, *2*, 55.
- (42) Förster, Th. *Comput. Biochem.* **1967**, *22*, 61.
- (43) Knoester, J. Incoherent energy transfer in disordered systems. Thesis University of Utrecht, Utrecht, 1987.
- (44) Scholes, G. D.; Clayton, H. A.; Ghiggionio, K. P. *J. Chem. Phys.* **1992**, *97*, 7405.
- (45) Ferguson, J. *J. Chem. Phys.* **1966**, *44* (7), 2677.
- (46) Karolin, J.; Johansson, L. B.-Å.; Ring, U.; Langhals, H. *Spectrochim. Acta A* **1996**, *52*, 747.
- (47) Kasai, H.; Kamatani, H.; Okada, S.; Oikawa, H.; Matsuda, H. *Jpn. J. Appl. Phys.* **1996**, *35*, L221.
- (48) Kimura, K.; Yamazaki, T.; Katsuma, S. *J. Phys. Chem.* **1971**, *75*, 5 (12), 1768–1774.
- (49) Vitukhnovski, A. G.; Sluch, M. I.; Warren, J. G.; Petty, M. C. *Chem. Phys. Lett.* **1991**, *184* (1, 2, 3), 235.
- (50) van Zandvoort, M. A. M. J.; Wróbel, D.; Lettinga, P.; van Ginkel, G.; Levine, Y. K. *Photochem. Photobiol.* **1995**, *62*, 279.
- (51) van Zandvoort, M. A. M. J.; Wróbel, D.; Lettinga, P.; van Ginkel, G.; Levine, Y. K. *Photochem. Photobiol.* **1995**, *62*, 299.